inorganics

MDPI

Article

Cobalt Protoporphyrin IX Attenuates Antibody-Mediated, Complement-Dependent Podocyte Injury: Role of Cobalt and Porphyrin Moieties

Elias A. Lianos [1,2,*], Gia Nghi Phung [1], Jianping Zhou [3] and Mukut Sharma [3,*]

[1] Salem Veterans Affairs Health Care System, Salem, VA 24153, USA; gia.phung@va.gov
[2] Department of Basic Science Education, Virginia Tech Carilion School of Medicine, Roanoke, VA 24016, USA
[3] Kansas City VA Medical Center, Kansas City, MO 64128, USA; jianping.zhou@va.gov
* Correspondence: elias.lianos@va.gov (E.A.L.); mukut.sharma@va.gov (M.S.); Tel.: +1-540-819-3543 (E.A.L.); +1-816-861-4700 (ext. 58222) (M.S.)

Abstract: Metalloporphyrins (MPs) that induce heme oxygenase (HO)-1 were shown to attenuate complement-mediated glomerular injury, with cobalt protoporphyrin IX (CoPPIX) being the most effective. To decipher the efficacy between CoPPIX and its constituents (Co, PPIX), we compared the outcomes of treatment with each in a rat model of complement-dependent immune injury of glomerular epithelial cells (podocytes). Outcomes were correlated with HO-1 induction and expression levels of complement C3 and of the complement activation regulators (CARs) cluster of differentiation (CD)55, CD59, and CR1-related gene y protein product (Crry). Podocyte injury was induced in rats following a single injection of the complement-fixing antibody against the podocyte antigen, Fx1A. CoPPIX or its constituents, cobaltous chloride ($CoCl_2$) and protoporphyrin IX (PPIX), were injected prior to and on alternate days thereafter. Urine was assessed for protein excretion and kidney cortex samples were processed for histopathology and assessment of target gene mRNA and protein levels using digital polymerase Chain Reaction (dPCR) and capillary-based Western blot analysis. The anti-Fx1A antibody caused proteinuria and podocyte injury. Treatment with the full CoPPIX chelate reduced proteinuria but treatment with either $CoCl_2$ or PPIX did not. CoPPIX treatment potently induced HO-1 and reduced tissue C3 mRNA and protein levels. It also increased CD55, CD59, and Crry mRNA, with an inconsistent effect on protein levels. The Co moiety was required for HO-1 induction but not for the decrease in C3. This decrease did not significantly correlate with the effects of CoPPIX treatment on CD55 protein levels. Chelation of cobalt to PPIX enhanced its potency to induce HO-1 but reduced that on CD55 induction. These observations distinguish between the effects of CoPPIX and its constituents on proteinuria consequent to complement-mediated podocyte injury and underlying mediators and identify this MP as a potential disease-modifying agent.

Keywords: immune injury; podocytes; hemoxygenase-1; complement activation regulators; cobalt chloride; cobalt protoporphyrin

Academic Editors: Wolfgang Linert and Carlos Martínez-Boubeta

Received: 2 November 2024
Revised: 17 February 2025
Accepted: 19 February 2025
Published: 23 February 2025

Citation: Lianos, E.A.; Phung, G.N.; Zhou, J.; Sharma, M. Cobalt Protoporphyrin IX Attenuates Antibody-Mediated, Complement-Dependent Podocyte Injury: Role of Cobalt and Porphyrin Moieties. *Inorganics* **2025**, *13*, 66. https://doi.org/10.3390/inorganics13030066

1. Introduction

Porphyrins are widely distributed in nature and have been extensively studied in terms of biomedical significance [1]. They are unique in that they contain a highly conjugated, heterocyclic macrocycle structure (porphyrin) comprised of four pyrrole subunits linked together by four methine bridges. The heterocyclic porphyrin core can coordinate with

various metal ions, thereby forming metalloporphyrins (MPs). The metal ion determines the functionality of MPs as well as their biological and metabolic effects [2]. For example, Fe-protoporphyrin IX (FePPIX) (heme) serves as an essential molecule in aerobic organisms, in which it controls gas exchange, mitochondrial energy production, antioxidant defense, and signal transduction. Moreover, it is a constituent of the superfamily of cytochromes in their role as oxidative, peroxidative, and reductive metabolism processes [3].

The observation that FePPIX plays a key role in enzyme function prompted the substitution of Fe to generate MPs containing other metals (Co, Zn, Sn, Cr, etc.) and the assessment of this intervention on enzyme function. This approach was further justified by the demonstration that exogenous administration of not only FePPIX but also non-iron PPs, such as cobalt (Co) PPIX, can be incorporated into human cytochrome P450 enzymes without significant perturbation in their overall protein structure [4]. Therefore, novel metalloporphyrin-based biocatalysts with the desired biological effect will likely be highly valuable for biomedical applications. To this end, FePPIX and CoPPIX have provided prototypic structures to develop porphyrin-based compounds.

The chelated metal ion in MPs determines their inductive or inhibitory effect on the synthesis and catalytic activity of heme oxygenase (HO). This enzyme catalyzes the degradation of FePPIX (heme) to biliverdin, ferrous iron (Fe^{2+}), and carbon monoxide (CO). Two major isoforms of HO (HO-1 and HO-2) exist in mammalian cells. HO-2 is constitutively expressed in most tissues. In contrast, HO-1 is the inducible isoform, and its expression is highly increased in response to different types of stress. It exerts antioxidant, cytoprotective and immunoregulatory effects in various disease states [5]. Seminal studies in the early eighties demonstrated that certain non-Fe MPs inhibit HO activity. Zinc, tin, and manganese protoporphyrin were found to be competitive HO inhibitors owing to a much higher binding activity than FePPIX to both HO-1 (the inducible HO isoform) and HO-2 (the constitutive HO isoform) [6,7]. In contrast to FePPIX, these non-Fe MPs are not oxidatively degraded because they have no oxygen-binding capacity. CoPPIX is unique in that it significantly inhibits HO activity in vitro [8] but enhances activity in vivo [4] due to its strong activation of HO-1 gene expression [9]. Of the CoPPIX constituents, protoporphyrin IX (PPIX) is an important precursor to biologically essential prosthetic groups such as heme, cytochrome c, and chlorophylls but does not induce HO. Cobalt (cobaltous chloride, $CoCl_2$) markedly induces HO, resulting in heme oxidation, and this effect was found to be more pronounced, albeit short-lived, than that of CoPPIX [10].

We previously reported that systemic administration of MPs with different metal functionalities reduced the severity of antibody-mediated, complement-dependent renal immune injury targeted to glomerular capillaries (glomeruli) and resulting in glomerular inflammation (glomerulonephritis). This was shown both in an aggressive model of injury resembling human rapidly progressive glomerulonephritis [11] and in a more indolent model resembling human membranous nephropathy [12]. Of the MPs employed in the latter model, CoPPIX treatment was the most effective in reducing proteinuria and inducing HO-1 in glomeruli. FePPIX (heme) was less effective, with minimal effect on HO-1 induction, while treatment with metal-devoid PPIX had minimal to no effect on proteinuria or on HO-1 expression [12].

Given the superior efficacy of CoPPIX in reducing proteinuria and the distinct biological effects of the full complex and its constituents, the present study sought to determine which constituent (Co, PPIX) accounts for the antiproteinuric effect of CoPPIX in the same rat model of complement-dependent podocyte immune injury that resembles human membranous nephropathy. Further, the effect of each constituent was correlated with HO-1 induction and with underlying mechanisms of injury, including complement activation and the expression of complement regulatory proteins.

2. Results

2.1. Effect of CoPPIX, PPIX, and $CoCl_2$ Treatment on Clinical Phenotype

Treatment with CoPPIX, PPIX, and $CoCl_2$ did not have an apparent effect on locomotor activity or cause an anxiety-like behavior. By day 14 (study endpoint), there was a statistically significant weight loss in rats injected with anti-Fx1A antibody (Ab) (Figure 1) compared to the controls. There was no further loss in body weight in rats injected with this Ab and treated with $CoCl_2$.

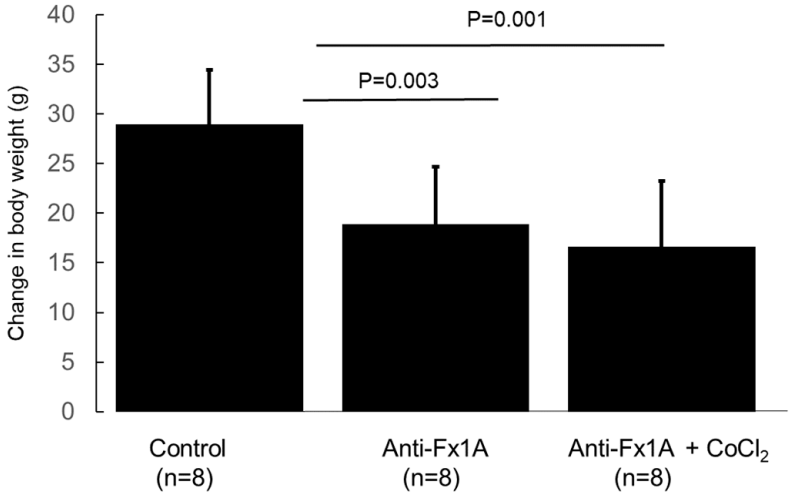

Figure 1. Changes in body weight following administration of anti-Fx1A immune serum (anti-Fx1A) without or with cobaltous chloride (anti-Fx1A + $CoCl_2$) treatment. Administration of anti-Fx1A serum caused a statistically significant loss in body weight by day 14 (study endpoint) compared to controls. There was no further loss in body weight in rats injected with this serum and treated with $CoCl_2$ (5 mg/Kg body weight; n = 8 each group, change in body weight (g) shown as mean ± SD).

The effect of CoPPIX, PPIX, and $CoCl_2$ treatments on protein excretion expressed as urine albumin to creatine ratio (ACR, mg/mg) or as total urine protein Up to urine creatinine (Uc) ratio (Up/Uc, mg/mg) is shown in Figure 2. CoPPIX treatment of rats with podocyte immune injury reduced ACR to levels not significantly different from the controls (Figure 2a). In PPIX or $CoCl_2$-treated rats with podocyte injury, the decrease in ARC or Up/Uc was not statistically different from those of non-treated animals (Figure 2b,c).

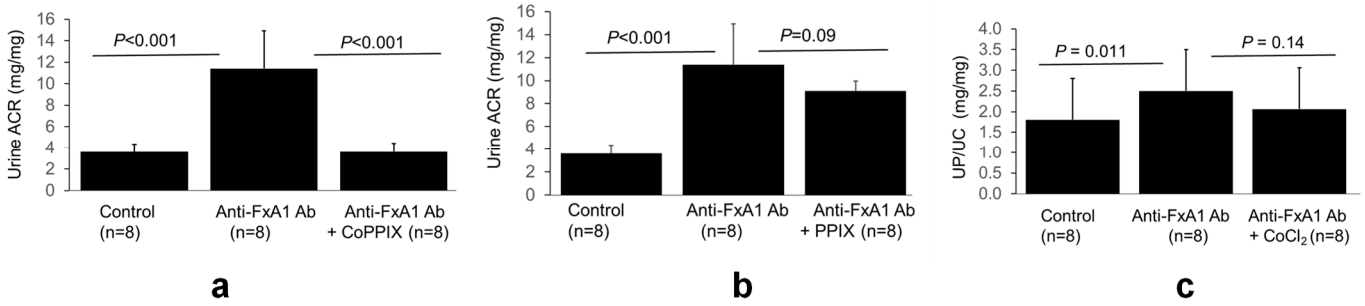

Figure 2. Effect of CoPPIX, PPIX, and $CoCl_2$ treatment on proteinuria. Urine protein excretion, expressed as urine albumin to creatine ratio (ACR, mg/mg) or as total urine protein Up to urine creatinine (Uc) ratio (Up/Uc) in cobalt protoporphyrin IX (CoPPIX), protoporphyrin IX (PPIX), and cobaltous chloride ($CoCl_2$)-treated rats with anti-FX1A immune serum-mediated podocyte injury. (**a**) CoPPIX treatment reduced ARC to a level that was no different from the control. (**b**,**c**) PPIX or $CoCl_2$ treatment did not significantly reduce proteinuria.

Histologically, there were glomerular lesions consistent with previously characterized glomerular pathology in this model [13,14]. Specifically, compared to the glomeruli of the control rats (Figure 3a), in the glomeruli of rats with anti-FX1A immune serum-induced podocyte injury, podocyte nuclei were enlarged (Figure 3b, encircled segment), and there was segmental hypercellularity with a mild increase mesangial matrix. In CoPPIX-treated rats, HO-1 was induced and immunolocalized in a minority of podocytes, as shown in a typical glomerular section (Figure 3c, arrowed cells) when compared to the number of podocytes identified as cells positive for the WT1 marker (cells with dark brown nuclei in Figure 3d).

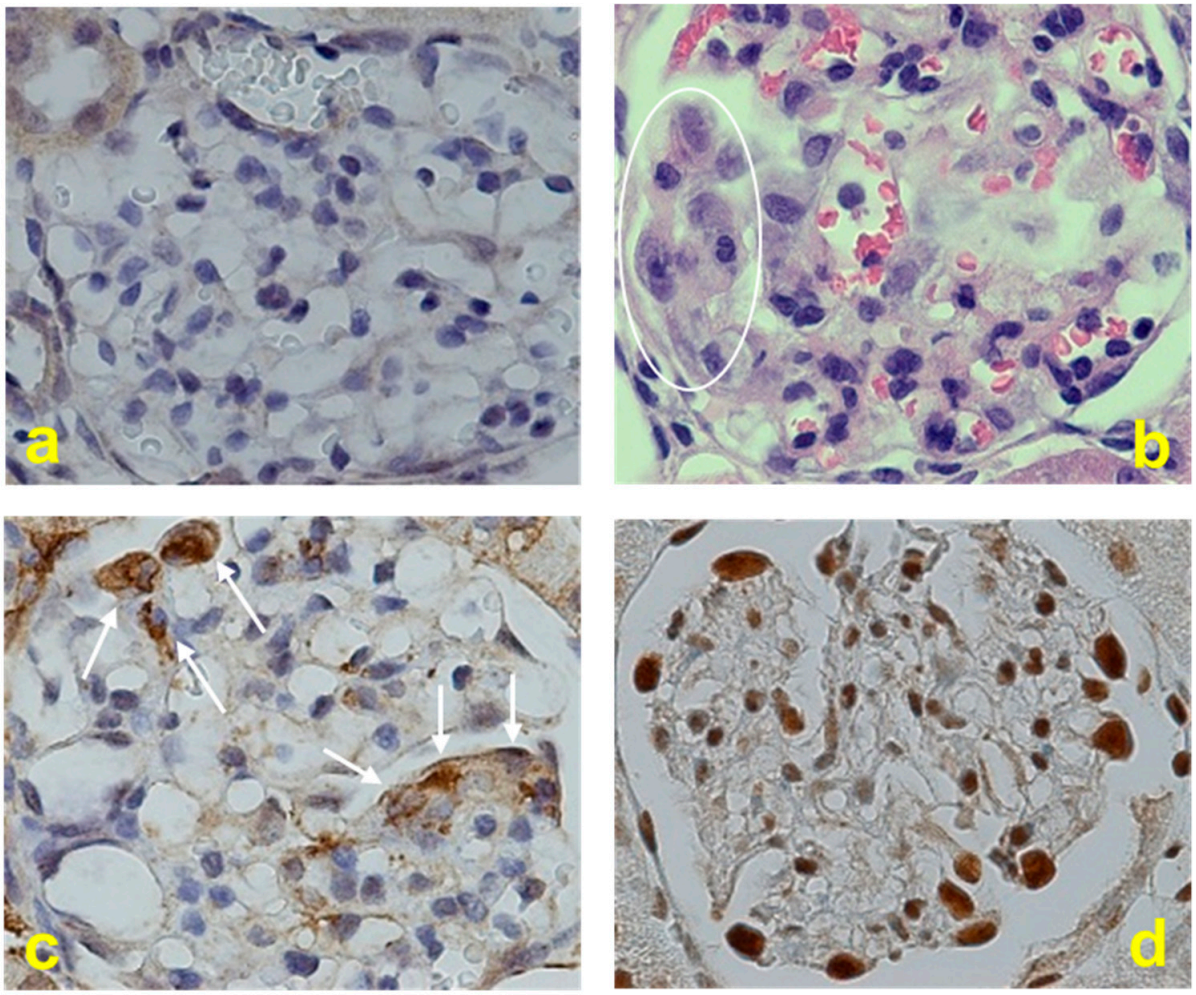

Figure 3. Micrographs of kidney cortical sections stained with Eosin/Hematoxylin (**a**,**b**) to assess glomerular morphology, the immunolocalization of HO-1 expression (**c**) and the immunolocalization of the podocyte marker, WT1 (**d**). All images were captured under 600× magnification.

2.2. HO-1 Protein Induction

As CoPPIX is a strong HO-1 inducer, we next assessed the magnitude of HO-1 induction in cortical tissue protein lysates in controls, in rats with anti-Fx1A antibody-mediated podocyte injury, and in CoPPIX-treated rats with podocyte injury. Capillary electrophoresis-based Western blot analysis of HO-1 induction revealed undetectable HO-1 protein in the control and in rats with podocyte immune injury but a robust induction in CoPPIX-treated rats with injury (Figure 4).

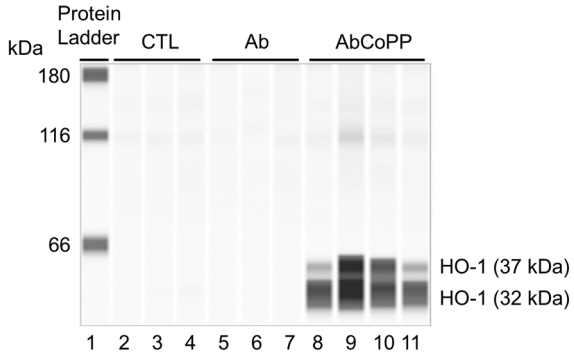

Figure 4. HO-1 protein levels determined using Western blot analysis of kidney cortex total protein lysates from control rats (CTL group, capillaries 2, 3, 4), from rats with anti-Fx1A antibody-mediated podocyte injury (Ab group, capillaries 5, 6, 7) and from CoPPIX-treated rats with podocyte injury (AbCoPP group, capillaries 8, 9, 10, 11). Total protein loaded for analysis was 16–20 pg.

2.3. Effect of CoPPIX, FePPIX, PPIX, and $CoCl_2$ Treatments on HO-1 Expression

Absolute quantification of changes in *HMOX1* gene expression (mRNA transcripts) in renal cortical tissue samples of rats with anti-Fx1A Ab mediated podocyte injury treated with CoPPIX, FePPIX, PPIX, and $CoCl_2$ was assessed using digital PCR (dPCR) performed as described in Section 4. A representative 1D dPCR scatterplot for the *HMOX1* gene is shown in Figure 5.

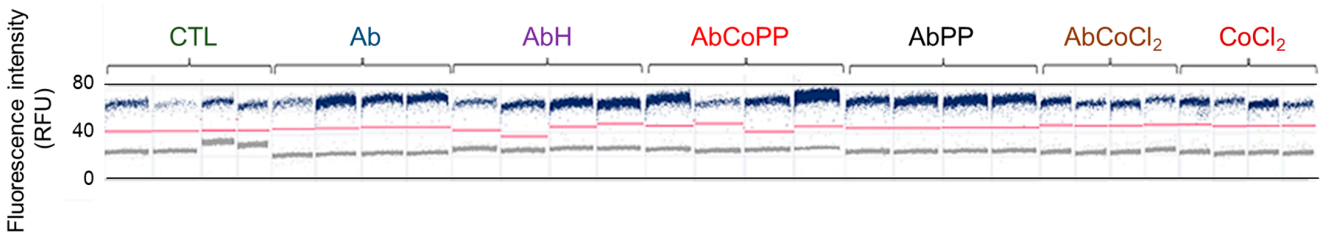

Figure 5. Relative fluorescence intensity of Hmox-1 mRNA in rat kidney cortex. One-dimensional scatterplot view of analyzed target gene (*HMOX1*) showing signals in positive and negative partitions of PCR reactions detecting *HMOX1* mRNA. Selected wells are displayed horizontally and separated by vertical columns. Signals are expressed as fluorescence intensity units (y-axis) and were generated by sequence-specific DNA probes. The TaqMan probes used in PCR reactions were FAM-MGB-labeled (green fluorophore-labeled dye), reflecting the fluorescence intensity obtained. Red horizontal lines represent the threshold fluorescence intensity value used to distinguish between positive (upper) and negative (lower) partitions. The x-axis represents analyzed partitions, while the y-axis represents the relative fluorescence intensity in each partition (8500 partitions per 24 or 96-well plate). Each blue dot in the Fluorescence Intensity Scatterplot represents 1 positive partition. Number of positive partitions is directly proportional to the mRNA concentration (copies/µL). Concentration (expressed in mRNA copy number/µL) is calculated based on positive and negative partitions. As the DNA template is partitioned randomly, Poisson statistics were used to calculate the amount of target DNA per positive partition. The total amount of target DNA in all partitions of a well was then calculated by multiplying the amount of target DNA per partition by the number of positive partitions. The calculation of the target gene concentration was determined by referring back to the volume in all analyzable partitions, i.e., partitions filled with the PCR reaction mix. The total number of filled partitions was identified by a fluorescent dye present in the reaction mix itself.

Podocyte immune injury induced by anti-Fx1A immune serum (Ab group) had no effect on HMOX1 mRNA levels compared to the controls (CTL group) (Figure 6). Of the two metalloporphyrins, CoPPIX treatment (AbCoPP group) caused a robust increase in *HMOX1* mRNA. In contrast, FePPIX (hemin, AbH group) and the metal-free PPIX (AbPP group) did not (Figure 6). $CoCl_2$ treatment also increased *HMOX1* mRNA in animals with podocyte immune injury (AbCoCl group) compared to controls or to animals with immune

injury not treated with $CoCl_2$ (Ab group). Likewise, the administration of $CoCl_2$ alone to a group of normal rats (CoCl group) significantly increased *HMOX1* mRNA compared to the control group (Figure 6). FePPIX (heme); moreover, CoPPIX administration is known to suppress aminolaevulinic acid synthase-1 (ALAS1) expression, the first and rate-limiting enzyme in the mammalian heme biosynthetic pathway, at transcriptional, translational, and post-translational levels [15,16]. To determine the effects of CoPPIX, FePPIX, PPIX, and $CoCl_2$ treatments employed on ALAS1 expression, *ALAS1* mRNA levels were measured in total RNA extracted from renal cortical tissue obtained from all treatment groups. As shown in Figure 6, *ALAS1* mRNA levels did not significantly change (relative to control) in any of the treatment groups, including those in which there was a significant increase in HO-1 expression (CoPPIX and CoCl groups).

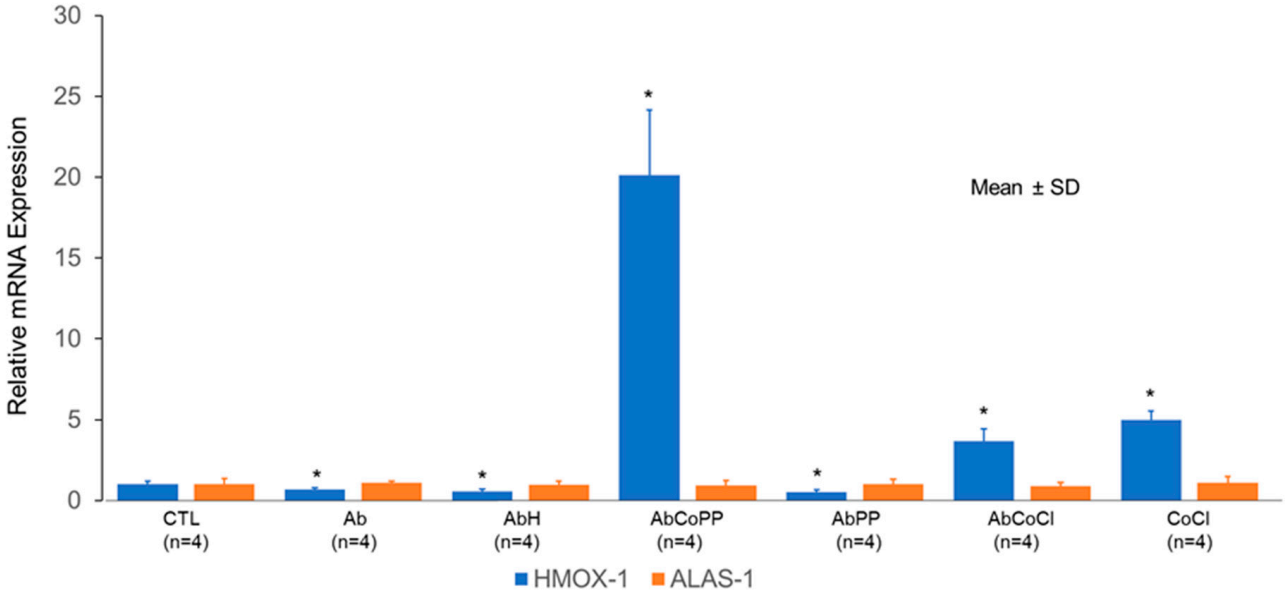

Figure 6. Changes in the **relative expression of *HMOX1* and *ALAS1* mRNA transcript levels in rat kidney cortical tissues.** Levels were expressed relative to those in the control group (taken as 1) as described in Section 4, and values are presented as means and standard deviations. Analysis of Variance (ANOVA) with post hoc pairwise comparisons using the Tukey–Kramer test was used to determine mean differences in mRNA levels across groups. CTL, Control group. Ab, rats injected with anti-Fx1A immune serum (Ab) only. AbH group, rats injected with anti-Fx1A immune serum and treated with Fe-protoporphyrin IX (FePPIX), also known as hemin (H). AbCoPP group, rats injected with anti-Fx1A immune serum and who received cobalt protoporphyrin IX (CoPPIX) treatment. AbPP group, rats injected with anti-Fx1A immune serum and who received metal-free protoporphyrin IX (PPIX) treatment. AbCoCl group, rats injected with anti-Fx1A immune serum and treated with cobaltous chloride. CoCl group, normal rats treated with cobaltous chloride only. *, indicates a significant increase or decrease compared to the control.

2.4. Assessment of CoPPIX, FePPIX, PPIX, and $CoCl_2$ Treatments on Expression (mRNA) of Complement (C3) and Complement Activation Regulators

Previous studies using the podocyte immune injury model employed in the present studies demonstrated that the binding of the anti-Fx1A antibody increases C3 synthesis through intrinsic glomerular cells [17]. This effect coincided with the onset and progression of proteinuria and peaked on days 11–14 [18]. We, therefore, assessed changes in mRNA levels of C3 and of specific complement activation regulators (CARs; CD55, CD59, Crry), shown to be expressed in podocytes [19], in response to the treatment protocols employed. Changes in kidney cortex mRNA levels of *C3*, *CD55*, *CD59*, and *Crry* in the control rats (CTL group, no immune injury), in rats with anti-Fx1A immune serum-induced podocyte

immune injury that received no treatment (Ab group), and in rats with immune injury that were treated with FePPIX (heme, H) (AbH group), CoPPIX (AbCoPP group), PPIX (AbPP group), or cobaltous chloride (AbCoCl group) are shown in Figure 7, in which changes in the mRNA levels of normal rats treated with cobaltous chloride alone (CoCl group) are also shown. mRNA concentrations (copies/μL) in each total RNA sample were factored by concentrations of GAPDH mRNA copies in the same sample. The mean value for each group was then compared to that of the control group, taken as 1 (relative expression). In rats with immune injury that received no treatment (Ab group), C3 mRNA levels increased relative to the control (CTL) group (Figure 7, panel A). These levels were significantly reduced in all groups with immune injury treated with FePPIX (AbH group), CoPPIX (AbCoPP group), PPIX (AbPP group), or $CoCl_2$ (AbCl group). In untreated rats with immune injury (Ab group), CD55 mRNA levels were reduced compared to those in controls (CTL group), while those of CD59 and Crry did not change (Figure 7, panels C and D). FePPIX treatment (AbH group) partially but not significantly reversed the reduction in CD55 mRNA levels, which remained significantly lower compared to controls (Figure 7, panel B). In contrast, both CoPPIX and $CoCl_2$ treatments (AbCoPP, AbCoCl groups) significantly reversed the reduction in CD55 mRNA to levels that were no different from controls (CTL). PPIX treatment (AbPP group) had no significant effect (Figure 7, panel B). Immune injury (Ab group) had no effect on CD59 mRNA levels (Figure 7, panel C). Except for the $CoCl_2$ treatment (AbCoCl group), all other treatments significantly increased CD59 mRNA (Figure 7, panel C). Crry mRNA levels did not change in rats with immune injury (Ab group) compared to controls (CTL group). In these, Crry mRNA increased significantly only in response to CoPPIX treatment (AbCoPP) (Figure 7, panel D).

Given the robust effect of CoPPIX treatment on HO-1 induction (Figure 4) coupled with reduced *C3* mRNA levels associated with increased levels of the complement regulators tested (CD55, CD59, Crry) (Figure 7), we next assessed the effect of this metalloporphyrin, its constituents (Co, PPIX), and of PPIX complexed to a different metal (Fe, FePPIX) on the directionality of changes in C3, HO-1, and CD55 protein levels in the lysates of kidney cortex. We focused on CD55 as HO-1 was shown to upregulate this complement activation regulator and decrease C3 when overexpressed in glomerular podocytes using a targeted transgenesis approach [19].

The results are shown in Figure 8, which demonstrates protein levels in tissue lysates analyzed using capillary electrophoresis-based Western blot analysis. C3 protein was present in lysates from control animals (panel a, CTL group, capillaries 2, 3, and 4), and levels increased in lysates from rats with immune injury (panel a, Ab group, capillaries 5, 6, and 7). In tissue lysates from FePPIX (hemin, H) and CoPPIX-treated animals (panel a, groups AbH and AbCoPP, capillaries 8–13), C3 protein decreased compared to the non-treated rats with injury (Ab group). $CoCl_2$ treatment (panel a, AbCoCl group, capillaries 17, 18, 19) also decreased C3 protein, albeit to a lesser degree compared to FePPIX and CoPPIX treatments. PPIX treatment (panel a, AbPP group, capillaries 14, 15, 16) had no effect. Only CoPPIX treatment caused a robust HO-1 induction (Figure 8, panel b, capillaries 11, 12, 13). FePPIX treatment had no effect on HO-1 (panel b, capillaries 8, 9, 10), while $CoCl_2$ treatment had a weak effect (panel b, capillaries 17, 18, 19) that was comparable to that of $CoCl_2$ administration to normal rats (panel b, capillaries 20, 21, 22). The decrease in C3 protein in FePPIX or CoPPIX-treated rats with immune injury (Figure 8, panel a, lanes 8–13) was not associated with a significant change in CD55 protein levels (Figure 8, panel c, capillaries 8–13). $CoCl_2$ treatment of normal rats (no immune injury) significantly increased CD55 protein (Figure 8, panel c, capillaries 20, 21, 22).

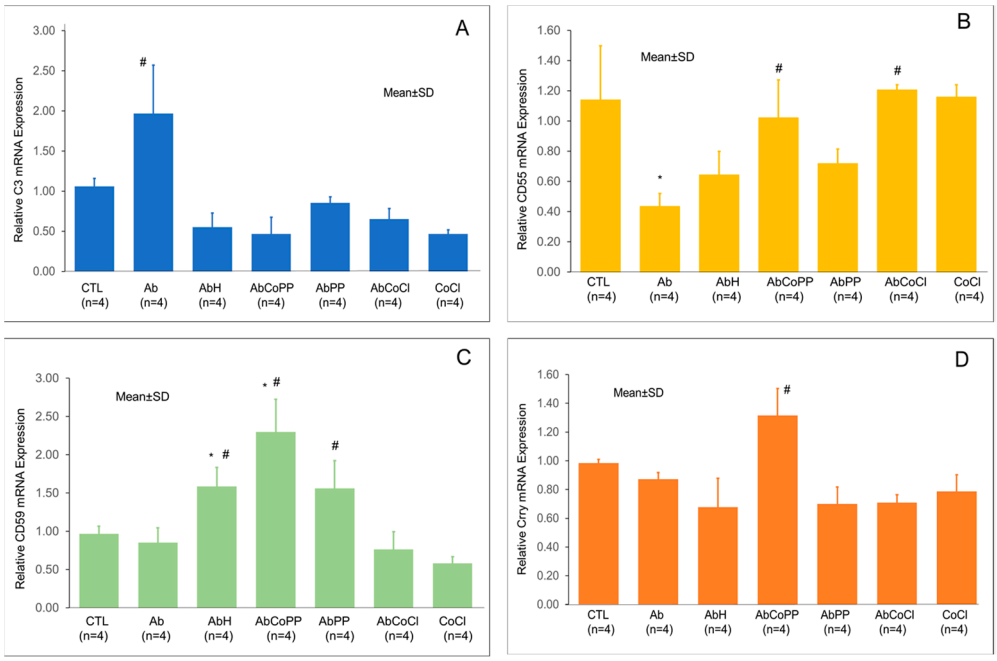

Figure 7. Effect of treatment of rats with podocyte immune injury on expression levels (mRNA) of *C3, CD55, CD59, and Crry* in whole cortex assessed using dPCR. Values are expressed as means and standard deviations. Analysis of Variance (ANOVA) was used to determine mean differences in mRNA levels across groups. Post hoc pairwise comparisons were performed using Tukey–Kramer's tests. Panel (**A**): In rats with immune injury (Ab group), cortical *C3* mRNA levels increased compared to controls (CTL group). This effect was reversed in all treatment groups (AbH, AbCoPP, AbCoCl). #, indicates a significant difference between the Ab group and all other groups. Panel (**B**): In rats with immune injury (Ab group), *CD55* mRNA was significantly reduced compared to the CTL group (indicated by *). FePPIX treatment (AbH group) partially but not significantly reversed *CD55* mRNA reduction, and levels remained significantly lower compared to controls (CTL). Both CoPPIX and $CoCl_2$ treatments (AbCoPP, AbCoCl groups) significantly reversed *CD55* reduction compared to the Ab group (indicated by #) to levels that were no different from the controls. PPIX treatment (AbPP group) had no significant effect. Panel (**C**): Immune injury (Ab group) had no effect on *CD59* mRNA levels compared to controls. Treatment of rats with immune injury with FePPIX (AbH group), CoPPIX (AbCoPP group), or PPIX (AbPP group) significantly increased *CD59* mRNA (indicated by #) compared to untreated animals (Ab group) and to the control group (indicated by *). $CoCl_2$ treatment (AbCoCl group) had no effect. Panel (**D**): Immune injury (Ab group) had no effect on cortical *Crry* mRNA levels compared to controls (CTL group). *Crry* mRNA in rats with immune injury increased significantly (indicated by #) only in response to CoPPIX treatment (AbCoPP group).

Taken together, these data indicate that the decrease in complement protein C3 in both CoPPIX and FePPIX-treated rats occurred independently of the magnitude of HO-1 induction and without significant effect on CD55 protein levels. Further, the robust HO-1 induction in CoPPIX-treated rats was not associated with a significant increase in CD55 protein.

Changes in the protein levels of the complement activation regulatory factors, CD59 and Crry, in cortical tissue protein lysates using Western blot analysis in response to FePPIX, CoPPIX, PPIX, or $CoCl_2$ treatments did not correlate with those in their mRNA levels and were inconclusive.

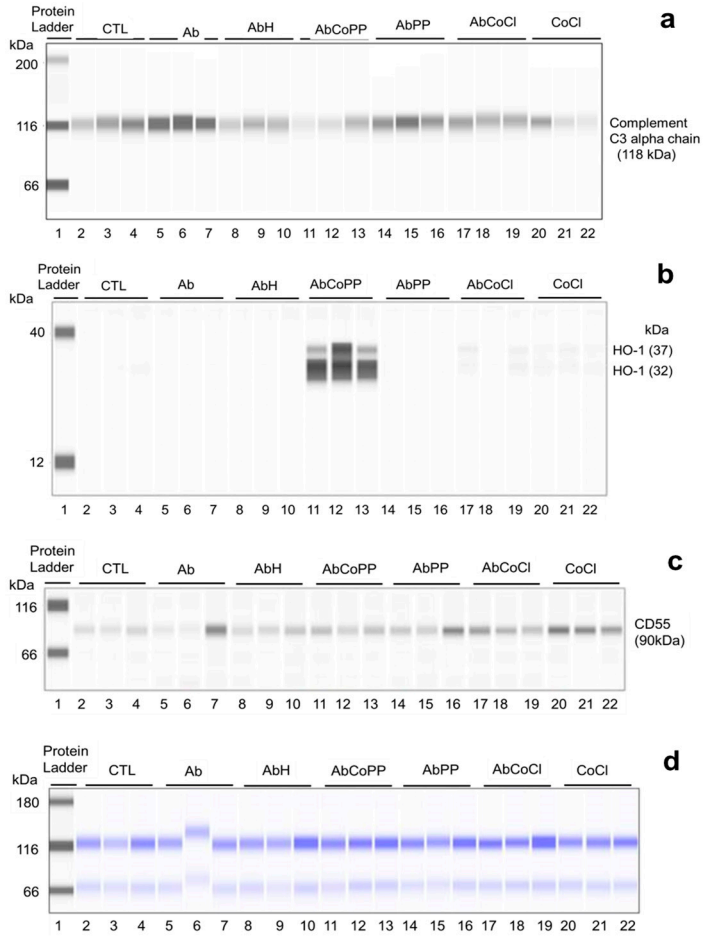

Figure 8. Capillary electrophoresis-based Western blot analysis of C3 (**a**), HO-1 (**b**), CD55 (**c**), and total protein (**d**) of lysates (16–20 pg total protein loaded in each capillary) obtained from the whole kidney cortex of treatment groups. CTL, control group. Ab, rats injected with anti-Fx1A immune serum (Ab) only. AbCoPP group, rats injected with anti-Fx1A immune serum (Ab) and who received cobalt protoporphyrin IX (CoPPIX) treatment. AbH group, rats injected with anti-Fx1A immune serum (Ab) and who received iron (Fe) protoporphyrin IX (FePPIX), also known as hemin (H), treatment. AbPP group, rats injected with anti-Fx1A immune serum (Ab) and treated with metal-free protoporphyrin IX (PPIX). AbCoCl group, rats injected with anti-Fx1A immune serum (Ab) and who received cobaltous chloride ($CoCl_2$) treatment. CoCl group, normal rats treated with $CoCl_2$ only. (**a**) Compared to untreated rats with immune injury (CTL group, capillaries 2, 3, 4), C3 protein levels increased in lysates from rats with podocyte immune injury (Ab group, capillaries 5, 6, 7). Treatment with either FePPIX or CoPPIX attenuated this increase (capillaries 8–13). $CoCl_2$ treatment (AbCoCl group) also decreased C3 but had a weaker effect. PPIX treatment (AbPP group) had no effect. (**b**) Only CoPPIX treatment caused a robust HO-1 induction (capillaries 11, 12, 13). FePPIX (hemin, H) treatment (AbH group, capillaries 8, 9, 10) had no appreciable effect, while $CoCl_2$ treatment (AbCoCl group, capillaries 17, 18, 19) had a weak effect that was comparable to that of $CoCl_2$ administration to normal rats (capillaries 20, 21, 22). PPIX treatment (AbPP group, capillaries 14, 15, 16) had no effect. (**c**) An increase in CD55 occurred only in normal rats (no podocyte immune injury) treated with Co not chelated to PPIX (CoCl group, capillaries 20, 21, 22).

3. Discussion

The present study was undertaken to further characterize the beneficial effects of metalloporphyrin (MP) treatment in experimental antibody-mediated, complement-dependent kidney injury. In addition to its localization in microvilli of the proximal tubular brush border, the Fx1A antigen, against which the immune serum employed was raised, is also localized in coated pits of the glomerular podocyte cell membrane [20]. Following the bind-

ing of the anti-Fx1A antibody, there is complement fixation in both podocytes and proximal tubular epithelial cells and assembly of complement proteins known to cause cell injury and increased permeability of glomerular capillaries to protein [13]. C3 and C5b-9 (also known as the membrane attack complex, MAC) are frequently detected with a distribution pattern similar to that of anti-Fx1A antibody binding. On the other hand, the cell membrane-bound complement activation regulatory proteins CD55 (decay-accelerating factor, DAF) and CD59 were shown to attenuate complement activation and the extent of injury. CD55 inhibits the formation of the C3 and C5 convertase enzymes of the classical and alternative activation pathways. CD59 inhibits the late stages of MAC formation by blocking the insertion of C9 in this complex [21]. Of the target cells to which the anti-Fx1A antibody binds, podocytes are terminally differentiated cells (restricted in a post-mitotic state) with limited ability to repair or regenerate following injury. This renders them vulnerable, and their loss has been linked to the progression of injury to chronic kidney disease in clinical and experimental studies. Examples of kidney diseases attributed to direct podocyte injury include minimal change disease, membranous nephropathy, focal segmental glomerular sclerosis, diabetic nephropathy, and HIV-associated nephropathy. Therefore, podocytes have been viewed as a promising target for the treatment of glomerular disease [22].

As podocytes are a key component of the glomerular capillary permeability barrier to circulating proteins, the assessment of urine albumin or total protein excretion has become an established marker of injury. Using this marker, we previously demonstrated that administration of metalloporphyrins (MPs) with different metal moieties (iron or cobalt protoporphyrin IX (FePPIX, CoPPIX)) reduced proteinuria. CoPPIX had the highest efficacy and potency in inducing heme oxygenase (HO-1) and reducing complement deposition in glomeruli [12]. The administration of metal-free PPIX had minimal or no effects, suggesting that the metal (Co) moiety was essential. The present study provided further insights by assessing proteinuria and underlying mediators in rats with anti-Fx1A antibody-mediated podocyte injury treated with the full CoPPIX complex, its components (Co and PPIX), and with PPIX complexed to a different metal (FePPIX).

As a constituent of Vitamin B12, cobalt is considered an essential element, and approximately 85% of its content in the body is in the form of this vitamin. Cobalt metal particles are practically insoluble in water; however, solubilization is greatly increased in biological fluids because of the extensive binding of Co (II) ions to proteins. The mechanism (s) of Co ion transport through cell membranes is unknown, but a role for the natural resistance-associated macrophage protein 2 (NRAMP 2) has been proposed [23]. Earlier studies have shown that the administration of cobalt to rats has an erythropoietic action by increasing blood volume and erythrocyte mass. Underlying mechanisms include the upregulation of erythropoietin gene expression by stabilizing the hypoxia-inducible factor, HIF-α [24,25]. Cobalt administered as oral enteric coated cobaltous chloride ($CoCl_2$) at doses from 25 to 50 mg daily for up to two months has been used in the medical treatment of anemia in patients with end-stage kidney disease or in anephric patients with severely reduced or absent erythropoietin production by the kidneys [26]. In contrast to the erythropoietic effect of its salt form ($CoCl_2$), when Co metal is complexed to PPIX, it efficiently mobilizes myeloid cells into the peripheral circulation. Underlying mechanisms include the induction of the granulocyte colony-stimulating factor (G-CSF) and other cytokines, including IL-6, MCP-1, and the Interferon gamma-induced protein 10 (IP-10). This effect was shown to be largely independent of the Nrf-2/HO-1 axis [27]. The disparate effect of $CoCl_2$ and CoPPIX in mobilizing bone marrow blood cells (erythrocyte vs. myelocyte progenitors, respectively) is one example highlighting the role of cobalt in determining the biological effects of the CoPPIX chelate.

The $CoCl_2$ dosing protocol employed in the present study was based on reports showing no nephrotoxicity of doses ranging from 3 to 10mg $CoCl_2$/kg/day [28] as well as on considerations of differences in pharmacokinetics between inorganic cobalt and CoPPIX in Sprague–Dawley rats. Specifically, following $CoCl_2$ treatment, cobalt is found predominantly (>95%) in plasma, from which it is rapidly eliminated ($t_{1/2}$ ~25 h), while kidneys retain the highest levels of cobalt (1.5 μg/g tissue) 4 weeks post-treatment and are the main route of Co excretion from the body [29]. In contrast, CoPPIX has a much slower elimination rate ($t_{1/2}$ ~3 days). These pharmacokinetic profiles indicate that differences in biological potency can be expected from the naturally occurring metal atom when it is complexed within an organic moiety. In this regard, CoPPIX is unique in that it exerts an extremely prolonged (up to 4 weeks after a single dose) effect on HO activity. In contrast, its inorganic metal component, $CoCl_2$, causes a robust but transient HO induction during the first 48 h after treatment, after which HO levels revert toward control [30,31]. These observations could, in part, explain differences in the extent of HO-1 induction observed in rats with podocyte immune injury treated with CoPPIX or $CoCl_2$ (Figures 6 and 8).

The antibody (rabbit anti-rat Fx1A serum) employed to cause podocyte injury was administered as a single intravenous injection at a dose sufficient to cause proteinuria (Figure 2), consistent with previous reports in this model [13,14]. In previous studies that assessed the efficacy of MP treatment in attenuating anti-Fx1A antibody-mediated podocyte injury, we focused on the HO-1 induction and extent of complement deposition in isolated glomeruli [12]. The present studies were performed in whole kidney cortex sections because, as mentioned above, antigenic determinants to which the anti-Fx1A antibody binds are present not only in glomerular podocytes but also in the brush border of proximal tubular cells where binding of this antibody initiates complement activation and injury as well [14]. Therefore, present studies used the whole cortex to maximize the detection of changes in the expression of target genes and proteins in response to the treatment protocols employed.

While the CoPPIX treatment of rats with podocyte immune injury markedly reduced proteinuria, treatment with its components (PPIX or Co) had no significant effect (Figure 2), indicating that the use of the full CoPPIX chelate was necessary to achieve the antiproteinuric effect. CoPPIX treatment was also the most potent inducer of HO-1 mRNA and protein (Figures 6 and 8). Of its components, Co (administered as $CoCl_2$ salt) significantly increased *HMOX1* mRNA levels, although not to the extent achieved by the full complex (CoPPIX, Figure 6). In contrast, treatment with PPIX alone had no effect (Figure 6). The lack of a stimulatory effect of PPIX treatment on HO-1 is not surprising, as previous studies have also demonstrated that this metal-free PP was ineffective in altering HO activity in vivo [32]. On the other hand, HO-1 induction observed in $CoCl_2$-treated rats (Figure 6) was expected as the administration of cobaltous chloride to rats is known to cause a marked and rapid increase in microsomal HO activity [10]. Treatment with FePPIX, which is the natural substrate/inducer of HO, also failed to significantly induce HO-1 (Figures 6 and 8). A plausible explanation is the differences in pharmacokinetics and fate between FePPIX and CoPPIX. CoPPIX has a much slower elimination rate (3 days) compared with FePPIX (10 h), and, as mentioned earlier (*vide supra*), four weeks following a single CoPPIX dose, the kidney retains the highest levels of cobalt metal compared to other organs [30]. In contrast, FePPIX rapidly complexes with hemopexin and albumin and is transported to the liver, where it is degraded by HO to biliverdin and CO [33].

The aforementioned pharmacokinetic differences could explain the robust HO-1 induction in CoPPIX but not in FePPIX-treated animals, an observation that corroborates findings in a previous report on the same immune injury model in which, in contrast to CoPPIX, treatment with FePPIX did not significantly induce HO-1 in isolated glomeruli [12].

However, FePPIX treatment in those studies did reduce proteinuria, and this calls into question the role of HO-1 induction as a key or sole mechanism underlying the antiproteinuric effect of CoPPIX treatment. Differences in pharmacokinetic and elimination rates between CoPPIX and $CoCl_2$ could also explain why the former was more potent in inducing HO-1. Specifically, CoPPIX has a much slower elimination rate (3 days) in comparison to noncomplexed Co and exerts an extremely prolonged (up to 4 weeks after a single dose) effect on HO activity in treated animals [29,30].

Taken together, these observations demonstrate that treatment with the full CoPPIX chelate but not its components (PPIX or Co) is required to reduce proteinuria. HO-1 induction is most robust when CoPPIX is administered repeatedly in the course of podocyte immune injury. However, HO-1 induction may not play a key role in mediating the antiproteinuric effect of CoPPIX.

FePPIX (heme) and CoPPIX administration are known to suppress aminolaevulinic acid synthase-1 (ALAS1) expression, the first and rate-limiting enzyme in the mammalian heme biosynthetic pathway, at transcriptional, translational, and post-translational levels [12,13]. Further, increased levels of free cellular heme suppress ALAS1, and this negative feedback regulation involves heme-dependent ALAS1 degradation [34]. Tissue levels of ALAS1 expression have, therefore, been regarded as an index/marker of free intracellular heme. Metal ions were shown to control both the production and degradation of cellular "free" heme by regulating the synthesis of ALAS1 in a manner similar to the complete metalloporphyrin complex (i.e., FePPIX or CoPPIX). This effect indicates that it is not necessary for metal ions to be chelated in the porphyrin ring in order to regulate enzymes of heme synthesis (ALAS1) and heme oxidation by HO [35,36]. To assess the effect of treatment protocols employed on ALAS1 expression, we measured changes in ALAS1 mRNA levels. As shown in Figure 6, and contrary to expectations, these levels did not change significantly (relative to control) in treatment groups, including those in which there was a significant increase in HO-1 expression in response to CoPPIX and $CoCl_2$ treatment and, therefore, reduced intracellular free heme levels. A possible explanation is the observation that ALAS1 expression levels are normally extremely low, which makes it difficult to assess decreases below normal levels. Moreover, there is a well-characterized biphasic response (suppression followed by rebound) of ALAS1 synthesis in response to heme and, similarly, to metals, including cobalt [37]. It is, therefore, conceivable that oscillations in ALAS1 production consequent to the repeated administration of FePPIX, CoPPIX, and $CoCl_2$ employed in the present studies could have "masked" detectable changes in ALAS1 expression.

As mentioned earlier, complement activation plays a key role in causing injury following the binding of the anti-Fx1A antibody to podocytes and proximal tubular epithelial cells. Moreover, the binding of this antibody was shown to increase the synthesis of the complement components through intrinsic glomerular cells [17,18]. Of the membrane-bound complement activation regulatory factors shown to mitigate complement-dependent podocyte injury following the administration of anti-Fx1A antibody, CD55 expression in the rat nephron is restricted to podocytes [38]. CD59 and Crry are also expressed in podocytes; however, their expression is not restricted in these cells [39,40]. They are also present and functionally active in glomerular endothelial and mesangial cells, where Crry limits the activation of the alternative complement pathway in both cell types [41]. Importantly, Crry expression is prominent in renal tubules and interstitium, where it also plays a key role in mitigating complement activation [42].

C3 mRNA levels increased in rats with immune injury (Figure 7, panel A), and this was associated with a significant decrease of *CD55* mRNA, while CD59 and Crry mRNA levels did not change (Figure 7, panels B, C, and D). The decrease in CD55 but not CD59 or Crry

expression in rats with immune injury could be attributed to anti-Fx1A antibody-mediated podocyte injury, as the expression of CD55 in the rat nephron is restricted to these cells [38]. The increase in *C3* mRNA levels in rats with immune injury was reversed by all treatments, and this reversal can be multifactorial. In an aggressive model of antibody-mediated, complement-dependent, rapidly progressive glomerular immune injury, podocyte-targeted HO-1 induction upregulated the complement regulatory protein CD55 and reduced C3 [19]. In the present study (antibody-mediated, complement-dependent podocyte injury), HO-1 induction was achieved through the systemic administration of HO-1 inducers, of which CoPPIX was the most potent and increased HO-1 expression in podocytes (Figure 3c). In addition to reducing *C3* mRNA, CoPPIX treatment preserved those CD55 mRNA levels (Figure 7, panel B) and significantly increased those of CD59 and Crry (Figure 7, panels C and D). Whether the robust HO-1 induction by CoPPIX could account for its effects on CD55, CD59, and Crry is uncertain. Definitive evidence can only be obtained using HO-1-deficient rats. However, these rats are short-lived and develop lesions in glomeruli and interstitium associated with proteinuria [43]. This would make comparisons between wild-type and HO-1-deficient rats problematic because, in both, podocyte immune injury is induced, and CoPPIX treatment is applied.

The effect of the treatment with each of the CoPPIX components (Co, PPIX) on CD55, CD59, and Crry mRNA varied. Cobalt chloride ($CoCl_2$) treatment of rats with immune injury reduced *C3* mRNA levels and mimicked the effect of the full chelate only in preserving CD55 expression with no effect on CD59 or Crry (Figure 7, panels B, C, and D). PPIX treatment also reduced *C3* mRNA and mimicked the effect of the full chelate in preserving both CD55 and CD59 with no effect on Crry (Figure 7, panels B, C, and D). Effects of FePPIX treatment were similar to those of PPIX, indicating that the Fe moiety of the FePPIX chelate did not play a significant role in preserving CD55 and CD59 expression. Taken together, these observations indicate that PPIX rather than Co accounts for the broader effect of CoPPIX in upregulating complement regulatory factors. Further, the administration of the full CoPPIX chelate is not required to reverse the increase in C3 expression in rats with podocyte immune injury, as each component can also achieve this effect.

Directional changes in the C3 protein in response to FePPIX, CoPPIX, and $CoCl_2$ treatments were correlated with those of HO-1 and CD55 (Figure 8) because of the presence of regulatory interactions between HO-1, CD55, and complement activation reported previously [19,44]. Similar to *C3* mRNA, C3 protein increased in animals with immune injury (Ab group) compared to the controls (CTL group), while FePPIX, CoPPIX, and, to a lesser extent, $CoCl_2$ treatments reduced C3 protein levels (Figure 8a). The C3 protein reduction in FePPIX or CoPPIX-treated rats did not correlate with changes in HO-1 or CD55 proteins as HO-1 protein levels markedly increased only in response to CoPPIX treatment even though FePPIX treatment reduced the C3 protein as well (Figure 8b). Moreover, neither treatment increased CD55 protein (Figure 8c). In $CoCl_2$-treated animals, C3 protein reduction was less pronounced compared to that in the CoPPIX-treated group (Figure 8a). In contrast, CD55 induction was more potent (Figure 8c). Taken together, the effects of repeated $CoCl_2$, PPIX, and CoPPIX administration on HO-1 and CD55 protein indicate that while the PPIX moiety has no effect, cobalt chelated to PPIX markedly enhances the HO-1-inducing potency of this metal but reduces its potency to upregulate CD55. Interestingly, treatment of normal rats with $CoCl_2$ alone increased CD55 protein levels compared to the control rats without immune injury (CTL group) that did not receive $CoCl_2$ (Figure 8c). The underlying mechanism of CD55 induction by $CoCl_2$ is unknown. A likely mechanism is the well-established role of this metal as a hypoxia mimetic. As such, it was shown to increase the expression of the Hypoxia Inducible Factor (HIF)-α by preventing its degradation [45]. Moreover, HIF-α upregulates CD55 [46].

4. Materials and Methods

4.1. Induction of Glomerular Podocyte Immune Injury

Animal research protocols employed were reviewed and approved by the Institutional Animal Care and Use Committee (IACUC), Institutional Biosafety Committee/Safety Committee (IBC/SRSS), and Research and Development Committee (R&DC) of the Kansas City Veterans Affairs Medical Center. The animal protocol of the present study was MS 007. The rat model of podocyte immune injury, as well as procedures and numbers of animals, were critically vetted during a pre-start review by the IACUC, which includes a veterinarian, scientific peers, research compliance official, and community members. The review included the use and justification of the number of animals as guided by the 3Rs (Replacement, Reduction, and Refinement) rule, as well as the justification for the use of animals. The pathobiological complexity of the antibody-mediated, complement-dependent model of podocyte immune injury employed in the present study and the demonstration that, compared to other species, this form of injury is most reproducible in the rat [13,47] excluded the use of non-animal models such as podocyte cell culture.

Podocyte immune injury was induced in female Sprague–Dawley rats (150 to 175 g) by a single intravenous (tail vein) injection of proteinuric doses (400 μL/100 g body weight) of immune serum raised in rabbits against the rat kidney proximal tubular brush border antigenic complex, Fx1A, in which the major antigenic determinant is megalin (gp330) [20,48]. Fx1A was isolated according to established methods [49], and the rabbit immune serum against it was a generous gift from Dr. Ashok Singh (Vivastem Laboratories, Lombard, IL, USA).

Proteinuria develops predictably within 5 to 6 d after a single injection of anti-Fx1A antibody and results from podocyte injury induced by complement activation and assembly on the podocytes of the complement membrane attack complex, C5b-9, and other complement components of earlier stages of complement activation [50,51]. The histopathology and pathogenesis of this model resemble human membranous nephropathy. Specifically, immunofluorescence microscopy demonstrates a granular pattern of IgG and C3 deposition in glomerular capillary walls, as seen in human membranous nephropathy. Additionally, the redistribution of nephrin, a key podocyte structural and functional protein, and its dissociation from the actin cytoskeleton, as well as disruption of the podocyte slit diaphragm, are observed. Consequently, protein permeability of the glomerular capillary barrier increases [47], and a similar process was shown in human membranous nephropathy [52].

The anti-Fx1A serum was heat-inactivated (56 °C, 30 min) and centrifuged (13,000 rpm, 60 min at 4 °C) prior to a single intravenous tail injection. Evidence for podocyte injury was assessed by measuring urine protein in samples collected 48 h before administration of the immune serum and on day 14 thereafter. A commercially available kit specific for measuring rat urine protein to creatinine ratio (Abcam, #ab272539) was used, and this ratio was expressed in mg/mg.

4.2. Metalloporphyrin (CoPPIX, FePPIX, PIXX) and $CoCl_2$ Treatment and Tissue Retrieval

Protoporphyrin IX cobalt chloride (CoPPIX) (Sigma, Burlington, MA, USA, Cat# C1900), Ferri-protoporphyrin IX, (FePPIX) chloride (Sigma, Burlington, MA, USA, Cat# H9039), the metal-free protoporphyrin IX (PPIX, Sigma, Burlington MA, USA, Cat# H9039), and cobaltous chloride ($CoCl_2$, Sigma–Aldrich, St. Louis, MO, USA, Cat# 60818) were used as described below. FePPIX, dissolved in 0.1 N NaOH (pH 7.4 adjusted using 0.1 N HCl), was used after 1:10 dilution in saline (5 mg/Kg body weight). CoPPIX was dissolved in Dimethylsulfoxide (DMSO) and used at 5 mg/kg body weight. $CoCl_2$ (cobalt (II) chloride, anhydrous, ≥98.0% purity) was dissolved in saline and used at a final concentration of 5 mg/Kg body weight. $CoCl_2$ dosing was chosen based on studies showing that a dose

range of 3–10 mg $CoCl_2$/kg/day had no significant kidney toxicity [25] and had beneficial effects on endothelial function in an experimental model of diabetic nephropathy [53]. CoPPIX, FePPIX, PPIX, and $CoCl_2$ were injected intraperitoneally 24 h before administration of the anti-Fx1A serum and on days 1, 3, 6, and 10 thereafter. Animal body weight was measured before administration of the anti-Fx1A serum and at the termination of studies (day 14), at which point urine was also collected. Kidneys were harvested, and the kidney cortex was obtained for total protein or RNA extraction. Whole kidney cortex samples were obtained because, in addition to binding to glomerular podocytes, the anti-Fx1A Ab employed also binds to the brush border of proximal tubular cells, where it can also cause complement-dependent cytotoxic injury [11]. Total tissue protein or RNA extracts were obtained using previously described methods [54].

4.3. RNA Extraction and Assessment of Yield, Purity, and Integrity

Total tissue RNA was extracted using spin columns available in the RNeasy Plus Mini Kit (QIAGEN, Germantown, MD, USA). Genomic DNA (gDNA) was removed using gDNA Eliminator spin columns (QIAGEN) provided with the same kit. Following the manufacturer's instructions for total RNA purification, 10–20 mg of frozen rat kidney cortex tissue was dissected on dry ice and weighed. The tissue was disrupted and lysed in 350 µL of Buffer RLT Plus (QIAGEN), also provided with the kit, and containing 1% of β-mercaptoethanol/mL. To homogenize/lyse tissues, a disposable micropestle was used, followed by passing homogenate/lysate through a 21-gauge needle attached to a 3-mL syringe. The lysate was centrifuged for 3 min at maximum speed, and the supernatant was transferred to the gDNA Eliminator spin columns, which were centrifuged for 30 s at ≥10,000 rpm. The flow-through was mixed with 350 µL of 70% ethanol to precipitate the RNA, and the mixture was transferred to RNeasy spin columns and centrifuged at ≥10,000 rpm for 30 s. To perform the RNA wash step, 700 µL of RNeasy Wash 1 (RW1) buffer, (provided in the RNeasy Plus Mini Kit) was added to the RNeasy spin column, and the flow-through was discarded after centrifuging at ≥10,000 rpm for 30 s. Next, 500 µL of RNeasy elution buffer (RPE) (provided in the RNeasy Plus Mini Kit, QIAGEN, Germantown, MD, USA) was added to the column for a second wash step followed by a 30-s centrifugation at ≥10,000 rpm. The washing step with RPE Buffer was repeated with a 2-min centrifugation at ≥10,000 rpm. To eliminate any possible carryover of ethanol or residual flow-through, the RNeasy spin column was centrifuged for an additional 1 min at the recommended speed (12,000 rpm). For RNA elution, the RNeasy spin column was placed in a new 1.5 mL collection tube, and 30–50 µL of RNase-free water was added directly to the spin column membrane at room temperature for 1 min. RNA was eluted by centrifuging at ≥10,000 rpm for 1 min. Purified RNA was stored at −80 °C.

Extracted RNA concentration and purity were determined by measuring RNA absorbance in 10 mM Tris-Cl (pH 7.5) at 260 nm and 280 nm using the Synergy HTX Gen5 multimode reader (BioTek, Santa Clara, CA, USA) and the Take3 Trio microvolume plates for this instrument. The ratio of absorbance at 260 nm and 280 nm was used to assess RNA purity, and an A260/A280 ratio of 1.8–2.1 was considered an acceptable RNA purity level. RNA integrity was measured using a Qubit 4 Fluorometer (ThermoFisher Scientific, Waltham, MA, USA) and the Qubit RNA IQ Assay Kit (ThermoFisher Scientific, Waltham, MA, USA). The Qubit RNA IQ Assay utilized two dyes: one that binds to large and/or highly structured RNA and another that selectively binds to small, degraded RNA. RNA integrity and quality were assessed as an RNA IQ number, ranging from 1 to 10. A low RNA IQ number (values < 5) indicated RNA degradation and/or that the sample contained mainly small RNA fragments. A higher RNA IQ number indicated that the sample contained mainly large and intact RNA fragment structures.

4.4. Absolute Quantification of mRNA Levels Using Digital PCR (dPCR)

mRNA levels in total tissue RNA extracted were detected using the QIAcuity OneStep Advanced Probe Kit (QIAGEN, Germantown, MD, USA) combined with the QIAcuity One digital PCR System (QIAGEN). The QIAcuity OneStep probe kit allows reverse transcription and amplification of the mRNA of the target of interest in a single step without converting to cDNA. Following the manufacturer's instructions, each reaction sample was prepared according to Table S2 in the Supplement Section and the use of the relevant Nanoplate format. For each reaction sample, a master mix was prepared by adding 1× OneStep Advanced Probe Master Mix (4×), 1× OneStep Advanced Reverse Transcription (RT) Mix (100×), template RNA, RNase-free water, and 1× TaqMan FAM-MGB-labeled Gene Expression Assay (20×) (ThermoFisher Scientific, Waltham, MA, USA) specifically for rat species: Hmox-1 (Rn00561387_m1), ALAS-1 (Rn00577936_m1), Daf/CD55 (Rn00709472_m1), MAC-IP/CD59 (Rn00563929_m1), Complement component 3/C3 (Rn00566466_m1), Complement component receptor 1-like/Crry (Rn00570775_m1), (Rn00561646_m1), and reference gene GAPDH (Rn01775763_g1). Additional details on the dPCR reaction mix and primers used are provided in Supplement Tables S1 and S2.

To perform dPCR reactions, the RNA template was diluted 1:25 to detect CD59 and GAPDH mRNA or was used undiluted to detect CD55 and HMOX-1 mRNA. A reaction mixture (12 µL or 40 µL) was thoroughly mixed and transferred to either 8.5 k (24-well and 96-well) or 26 k (24-well) QIAcuity Nanoplate (QIAGEN, Germantown, MD, USA), respectively. The QIAcuity RT-dPCR thermal cycling program was set as follows: (I) reverse transcription (RT) at 50 °C for 30 min, (II) RT Enzyme Inactivation at 95 °C for 2 min, and (III) 40 cycles of denaturation at 95 °C for 15 sec followed by annealing and extension at 60 °C for 30 s. To assess the efficiency of dPCR reactions, a positive control assay was performed using Universal Rat Reference RNA (ThermoFisher Scientific, Waltham, MA, USA). Reactions containing a non-template control (NTC) or RNase-free water were also performed to check for dPCR reaction purity. The QIAcuity Software Suite 3.0 (QIAGEN) used the "green" detection channel (FAM-MGB) for fluorescent data analysis. Images were exposed for 500 ms with a gain of 6. The final absolute concentration of target mRNA (expressed as copies of target molecule per microliter) was calculated using the QIAcuity Software Suite 3.0 and the Poisson Distribution Law statistical method. In cases where samples saturated the reaction for some of the genes, resulting in expression levels too high to be accurately detected at the initial dilution, the reactions were repeated at a greater dilution. Results were expressed as changes in target gene mRNA copies in the various treatment groups relative to the control group. Specifically, target gene mRNA concentrations (copies/µL) in each total RNA sample were factored (normalized) by copies of GAPDH mRNA in the same sample. The mean mRNA concentration value for each group was then compared to that of the control group, which was taken as 1.

4.5. Capillary Electrophoresis-Based Separation and Immunodetection (Western Blot Analysis) of Tissue Proteins

A Western protein analyzer (ProteinSimple, Biotechne, Minneapolis, MN, USA) that performs protein separation, immunoprobing, chemiluminescence detection, total protein normalization, and data analysis was used. Protein lysate sample preparation/optimization, sample, and stacking matrix loading, assessment of a linear dynamic range of protein lysates to determine the limit of detection, optimization of dilution of antibodies employed, and assessment of protein loading were performed according to manufacturer's specifications/guidelines. The total protein loaded in each capillary was 16–20 pg, and individual proteins detected were factored (corrected) by the total protein loaded in each capillary using an in-capillary labeling technique whereby separated proteins are UV-captured in

the capillary wall in a manner similar to capturing target proteins. Captured proteins were biotin-labeled and detected using streptavidin-HRP in a chemiluminescent reaction. A total protein detection kit was used according to the manufacturer's (ProteinSimple, Biotechne, Minneapolis, MN, USA) specifications.

4.6. Antibodies Used

A mouse anti-rabbit IgG monoclonal antibody (Antibodies-online Inc., Pottstown, PA, USA) was used to detect the presence of the rabbit anti-rat Fx1A immune serum (exogenous Ig) injected. The detection levels of administered rabbit Ig in tissue protein lysates were used to select samples with similar Ig levels in analyzing the expression of proteins or genes of interest. The presence of complement component C3/C3b was detected using a mouse IgM monoclonal antibody (Ab) raised against an epitope on C3b that reacts with intact rat C3/C3b (HycultBiotech, Clone 2B10b9b2). HO-1 was detected using a rabbit polyclonal Ab raised against an HO-1/HMox1 fusion protein Ag1190 (Proteintech, Catalog# 10701-1-AP). To detect CD55, an anti-rat polyclonal antibody against a fragment (His-tag) corresponding to the 250aa of rat CD55 C-terminus (Abcam, catalog# ab231061) was used. To detect CD59, a polyclonal rabbit anti-rat CD55 Ab (ThermoFisher, Waltham, MA, USA, Cat# 117852) was used.

4.7. Data Analysis

Values are presented as means and standard deviations. The Analysis of Variance (ANOVA) method was used to explore mean differences in mRNA and protein levels across groups (control, immune injury, immune injury treated with either FePPIX, CoPPIX, PPIX, or cobaltous chloride compounds). Post hoc pairwise comparisons were then performed using the Tukey–Kramer test.

5. Conclusions

These studies demonstrate that in antibody-mediated, complement-dependent podocyte injury, the antiproteinuric effect of CoPPIX requires treatment with the full chelate as neither of its components (Co, PPIX) reduces urine protein excretion. CoPPIX treatment potently induces HO-1 and reduces C3 protein, the latter occurring independently of the extent of HO-1 induction or CD55 expression levels. It is, therefore, unlikely that HO-1 or CD55 are underlying mechanisms of C3 reduction. Chelation of cobalt to PPIX enhances the potency of this metal to induce HO-1 but reduces its potency on CD55 induction. This highlights a key role of this metal in determining CoPPIX effects on HO-1 and CD55 expression. In view of our previous and ongoing work, present results suggest a unique and beneficial role of cobalt in cobalt metalloprotoporphyrin. The role of CoPPIX as a potential therapeutic or disease-modifying agent in renal immune injury remains to be determined as CoPPIX treatment may have a number of side effects, including the depletion of hepatic cytochrome P450 levels [55], weight loss [56], and a reduction in serum thyroid and testicular hormone concentrations [57].

Supplementary Materials: The following supporting information can be downloaded at: https://www.mdpi.com/article/10.3390/inorganics13030066/s1, Table S1: Table of primers used; Table S2: Table summarizing reagents and volumes for dPCR.

Author Contributions: E.A.L.: Conceptualization, funding acquisition, project administration, supervision, writing, review, and editing. G.N.P., J.Z., and M.S.: Methodology, validation, and software. M.S.: Supervision, data curation, draft preparation, review, and editing. All authors have read and agreed to the published version of the manuscript.

Funding: This work was supported by a Veteran Affairs Merit Award 5I01BX004333-04, titled 'Novel Complement-targeted treatment strategies', awarded to Elias A. Lianos.

Institutional Review Board Statement: Animal experiments were performed following the relevant recommendations, guidelines, and regulations. Plan of work was approved by the Institutional Animal Care and Use Committee (IACUC), Institutional Biosafety Committee/Subcommittee on Research Safety (IBC/SRS), and the Research and Development (R&D) Committee at the VA Medical Center, Kansas City, MO, USA. This work was performed under protocol with Institutional Review Board number IRB 1619473-1 (MS0007) approved by the Kansas City VA Medical Center IACUC and renewed on 7 November 2024.

Informed Consent Statement: Not applicable.

Data Availability Statement: The original contributions presented in this study are included in the article/Supplementary Materials. Further inquiries can be directed to the corresponding author.

Acknowledgments: The views expressed in this article are those of the authors and do not necessarily reflect the position or policy of the Department of Veterans Affairs or the United States government. Alicia Lozano provided expert guidance on statistical analyses. Vassiliki Papavranousi posed critical questions and comments.

Conflicts of Interest: The authors declare no conflicts of interest. The funders had no role in the design of the study; in the collection, analyses, or interpretation of data; in the writing of the manuscript; or in the decision to publish the results.

References

1. Zhang, P.; Hu, J.; Liu, B.; Yang, J.; Hou, H. Recent advances in metalloporphyrins for environmental and energy applications. *Chemosphere* **2019**, *219*, 617–635. [CrossRef] [PubMed]
2. Ghosh, A.; Steene, E. High-valent transition metal centers and noninnocent ligands in metalloporphyrins and related molecules: A broad overview based on quantum chemical calculations. *J. Biol. Inorg. Chem.* **2001**, *6*, 739–752. [CrossRef] [PubMed]
3. Correia, M.A.; Sinclair, P.R.; De Matteis, F. Cytochrome P450 regulation: The interplay between its heme and apoprotein moieties in synthesis, assembly, repair, and disposal. *Drug Metab. Rev.* **2011**, *43*, 1–26. [CrossRef]
4. Yadav, R.; Scott, E.E. Endogenous insertion of non-native metalloporphyrins into human membrane cytochrome P450 enzymes. *J. Biol. Chem.* **2018**, *293*, 16623–16634. [CrossRef] [PubMed]
5. Facchinetti, M.M. Heme-Oxygenase-1. *Antioxid. Redox Signal* **2020**, *32*, 1239–1242. [CrossRef]
6. Maines, M.D. Zinc · protoporphyrin is a selective inhibitor of heme oxygenase activity in the neonatal rat. *Biochim. Biophys. Acta* **1981**, *673*, 339–350. [CrossRef]
7. Drummond, G.S.; Kappas, A. Prevention of neonatal hyperbilirubinemia by tin protoporphyrin IX, a potent competitive inhibitor of heme oxidation. *Proc. Natl. Acad. Sci. USA* **1981**, *78*, 6466–6470. [CrossRef]
8. Yoshinaga, T.; Sassa, S.; Kappas, A. Purification and properties of bovine spleen heme oxygenase. Amino acid composition and sites of action of inhibitors of heme oxidation. *J. Biol. Chem.* **1982**, *257*, 7778–7785. [PubMed]
9. Shan, Y.; Lambrecht, R.W.; Donohue, S.E.; Bonkovsky, H.L. Role of Bach1 and Nrf2 in up-regulation of the heme oxygenase-1 gene by cobalt protoporphyrin. *FASEB J.* **2006**, *20*, 2651–2653. [CrossRef]
10. Maines, M.D.; Kappas, A. Cobalt stimulation of heme degradation in the liver. Dissociation of microsomal oxidation of heme from cytochrome P-450. *J. Biol. Chem.* **1975**, *250*, 4171–4177. [CrossRef]
11. Datta, P.K.; Duann, P.; Lianos, E.A. Long-term effect of heme oxygenase (HO)-1 induction in glomerular immune injury. *J. Lab. Clin. Med.* **2006**, *147*, 150–155. [CrossRef]
12. Lianos, E.A.; Phung, G.N.; Foster, M.; Zhou, J.; Sharma, M. Metalloporphyrins Reduce Proteinuria in Podocyte Immune Injury: The Role of Metal and Porphyrin Moieties. *Int. J. Mol. Sci.* **2023**, *24*, 12777. [CrossRef] [PubMed]
13. Cybulsky, A.V.; Quigg, R.J.; Salant, D.J. Experimental membranous nephropathy redux. *Am. J. Physiol. Renal Physiol.* **2005**, *289*, F660–F671. [CrossRef]
14. Mendrick, D.L.; Noble, B.; Brentjens, J.R.; Andres, G.A. Antibody-mediated injury to proximal tubules in Heymann nephritis. *Kidney Int.* **1980**, *18*, 328–343. [CrossRef]
15. Kaasik, K.; Lee, C.C. Reciprocal regulation of haem biosynthesis and the circadian clock in mammals. *Nature* **2004**, *430*, 467–471. [CrossRef] [PubMed]
16. Zheng, J.; Shan, Y.; Lambrecht, R.W.; Donohue, S.E.; Bonkovsky, H.L. Differential regulation of human ALAS1 mRNA and protein levels by heme and cobalt protoporphyrin. *Mol. Cell Biochem.* **2008**, *319*, 153–161. [CrossRef]

17. Sasaki, O.; Zhou, W.; Miyazaki, M.; Abe, K.; Koji, T.; Verroust, P.; Tsukasaki, S.; Ozono, Y.; Harada, T.; Nakane, P.K.; et al. Intraglomerular C3 synthesis in rats with passive Heymann nephritis. *Am. J. Pathol.* **1997**, *151*, 1249–1256.
18. Zhou, W.; Andrews, P.A.; Wang, Y.; Wolff, J.; Pratt, J.; Hartley, B.R.; Verroust, P.; Sacks, S.H. Evidence for increased synthesis of complement C4 in the renal epithelium of rats with passive Heymann nephritis. *J. Am. Soc. Nephrol.* **1997**, *8*, 214–222. [CrossRef] [PubMed]
19. Detsika, M.G.; Duann, P.; Atsaves, V.; Papalois, A.; Lianos, E.A. Heme Oxygenase 1 Up-Regulates Glomerular Decay Accelerating Factor Expression and Minimizes Complement Deposition and Injury. *Am. J. Pathol.* **2016**, *186*, 2833–2845. [CrossRef]
20. Kerjaschki, D.; Farquhar, M.G. Immunocytochemical localization of the Heymann nephritis antigen (GP330) in glomerular epithelial cells of normal Lewis rats. *J. Exp. Med.* **1983**, *157*, 667–686. [CrossRef]
21. Morgan, B.P.; Meri, S. Membrane proteins that protect against complement lysis. *Springer Semin. Immunopathol.* **1994**, *15*, 369–396. [CrossRef] [PubMed]
22. Mallipattu, S.K.; He, J.C. The podocyte as a direct target for treatment of glomerular disease. *Am. J. Physiol. Renal Physiol.* **2016**, *311*, F46–F51. [CrossRef] [PubMed]
23. Forbes, J.R.; Gros, P. Iron, manganese, and cobalt transport by Nramp1 (Slc11a1) and Nramp2 (Slc11a2) expressed at the plasma membrane. *Blood* **2003**, *102*, 1884–1892. [CrossRef] [PubMed]
24. Taylor, A.; Brown, S.S.; International Union of Pure Applied Chemistry; Commission on Toxicology. Clinical chemistry and chemical toxicology of metals. In *Proceedings of the First International Symposium on Developments in Toxicology and Environmental Science*; Elsevier/North-Holland: New York, NY, USA, 1977; Volume 1, pp. 105–108.
25. Göpfert, T.; Eckardt, K.U.; Gess, B.; Kurtz, A. Cobalt exerts opposite effects on erythropoietin gene expression in rat hepatocytes in vivo and in vitro. *Am. J. Physiol.* **1995**, *269*, R995–R1001. [CrossRef] [PubMed]
26. Duckham, J.M.; Lee, H.A. The treatment of refractory anaemia of chronic renal failure with cobalt chloride. *Q. J. Med.* **1976**, *45*, 277–294.
27. Szade, A.; Szade, K.; Nowak, W.N.; Bukowska-Strakova, K.; Muchova, L.; Gońka, M.; Żukowska, M.; Cieśla, M.; Kachamakova-Trojanowska, N.; Rams-Baron, M.; et al. Cobalt protoporphyrin IX increases endogenous G-CSF and mobilizes HSC and granulocytes to the blood. *EMBO Mol. Med.* **2019**, *11*, e09571. [CrossRef]
28. Liu, Y.K.; Xu, H.; Liu, F.; Tao, R.; Yin, J. Effects of serum cobalt ion concentration on the liver, kidney and heart in mice. *Orthop. Surg.* **2010**, *2*, 134–140. [CrossRef]
29. Rosenberg, D.W. Pharmacokinetics of cobalt chloride and cobalt-protoporphyrin. *Drug Metab. Dispos.* **1993**, *21*, 846–849. [CrossRef] [PubMed]
30. Kirchgessner, M.; Reuber, S.; Kreuzer, M. Endogenous excretion and true absorption of cobalt as affected by the oral supply of cobalt. *Biol. Trace Elem. Res.* **1994**, *41*, 175–189. [CrossRef] [PubMed]
31. Drummond, G.S.; Kappas, A. The cytochrome P-450-depleted animal: An experimental model for in vivo studies in chemical biology. *Proc. Natl. Acad. Sci. USA* **1982**, *79*, 2384–2388. [CrossRef] [PubMed]
32. Maines, M.D.; Cohn, J. Bile pigment formation by skin heme oxygenase: Studies on the response of the enzyme to heme compounds and tissue injury. *J. Exp. Med.* **1977**, *145*, 1054–1059. [CrossRef] [PubMed]
33. Siegert, S.W.; Holt, R.J. Physicochemical properties, pharmacokinetics, and pharmacodynamics of intravenous hematin: A literature review. *Adv. Ther.* **2008**, *25*, 842–857. [CrossRef] [PubMed]
34. Kubota, Y.; Nomura, K.; Katoh, Y.; Yamashita, R.; Kaneko, K.; Furuyama, K. Novel Mechanisms for Heme-dependent Degradation of ALAS1 Protein as a Component of Negative Feedback Regulation of Heme Biosynthesis. *J. Biol. Chem.* **2016**, *291*, 20516–20529. [CrossRef]
35. Maines, M.D.; Kappas, A. Regulation of heme pathway enzymes and cellular glutathione content by metals that do not chelate with tetrapyrroles: Blockade of metal effects by thiols. *Proc. Natl. Acad. Sci. USA* **1977**, *74*, 1875–1878. [CrossRef] [PubMed]
36. Maines, M.D.; Kappas, A. Metals as regulators of heme metabolism. *Science* **1977**, *198*, 1215–1221. [CrossRef] [PubMed]
37. Waxman, A.D.; Collins, A.; Tschudy, D.P. Oscillations of hepatic delta-aminolevulinic acid synthetase produced in vivo by heme. *Biochem. Biophys. Res. Commun.* **1966**, *24*, 675–683. [CrossRef] [PubMed]
38. Bao, L.; Spiller, O.B.; St John, P.L.; Haas, M.; Hack, B.K.; Ren, G.; Cunningham, P.N.; Doshi, M.; Abrahamson, D.R.; Morgan, B.P.; et al. Decay-accelerating factor expression in the rat kidney is restricted to the apical surface of podocytes. *Kidney Int.* **2002**, *62*, 2010–2021. [CrossRef] [PubMed]
39. Quigg, R.J.; Holers, V.M.; Morgan, B.P.; Sneed, A.E. Crry and CD59 regulate complement in rat glomerular epithelial cells and are inhibited by the nephritogenic antibody of passive Heymann nephritis. *J. Immunol.* **1995**, *154*, 3437–3443. [CrossRef] [PubMed]
40. Cunningham, P.N.; Hack, B.K.; Ren, G.; Minto, A.W.; Morgan, B.P.; Quigg, R.J. Glomerular complement regulation is overwhelmed in passive Heymann nephritis. *Kidney Int.* **2001**, *60*, 900–909. [CrossRef]
41. Quigg, R.J.; Morgan, B.P.; Holers, V.M.; Adler, S.; Sneed, A.E.; Lo, C.F. Complement regulation in the rat glomerulus: Crry and CD59 regulate complement in glomerular mesangial and endothelial cells. *Kidney Int.* **1995**, *48*, 412–421. [CrossRef] [PubMed]

42. Thurman, J.M.; Ljubanović, D.; Royer, P.A.; Kraus, D.M.; Molina, H.; Barry, N.P.; Proctor, G.; Levi, M.; Holers, V.M. Altered renal tubular expression of the complement inhibitor Crry permits complement activation after ischemia/reperfusion. *J. Clin. Invest.* **2006**, *116*, 357–368. [CrossRef] [PubMed]
43. Atsaves, V.; Detsika, M.G.; Poulaki, E.; Gakiopoulou, H.; Lianos, E.A. Phenotypic characterization of a novel HO-1 depletion model in the rat. *Transgenic Res.* **2017**, *26*, 51–64. [CrossRef] [PubMed]
44. Lianos, E.A.; Wilson, K.; Goudevenou, K.; Detsika, M.G.; Sharma, M. Constitutive HO-1 and CD55 (DAF) Expression and Regulatory Interaction in Cultured Podocytes. *Biomedicines* **2023**, *11*, 3297. [CrossRef] [PubMed]
45. Yuan, Y.; Hilliard, G.; Ferguson, T.; Millhorn, D.E. Cobalt inhibits the interaction between hypoxia-inducible factor-alpha and von Hippel-Lindau protein by direct binding to hypoxia-inducible factor-alpha. *J. Biol. Chem.* **2003**, *278*, 15911–15916. [CrossRef]
46. Cimmino, F.; Avitabile, M.; Pezone, L.; Scalia, G.; Montanaro, D.; Andreozzi, M.; Terracciano, L.; Iolascon, A.; Capasso, M. CD55 is a HIF-2α marker with anti-adhesive and pro-invading properties in neuroblastoma. *Oncogenesis* **2016**, *5*, e212. [CrossRef] [PubMed]
47. Saran, A.M.; Yuan, H.; Takeuchi, E.; McLaughlin, M.; Salant, D.J. Complement mediates nephrin redistribution and actin dissociation in experimental membranous nephropathy. *Kidney Int.* **2003**, *64*, 2072–2078. [CrossRef] [PubMed]
48. Kerjaschki, D.; Ullrich, R.; Diem, K.; Pietromonaco, S.; Orlando, R.A.; Farquhar, M.G. Identification of a pathogenic epitope involved in initiation of Heymann nephritis. *Proc. Natl. Acad. Sci. USA* **1992**, *89*, 11179–11183. [CrossRef] [PubMed]
49. Edgington, T.S.; Glassock, R.J.; Dixon, F.J. Autologous immune complex nephritis induced with renal tubular antigen. I. Identification and isolation of the pathogenetic antigen. *J. Exp. Med.* **1968**, *127*, 555–572. [CrossRef]
50. Cybulsky, A.V.; Rennke, H.G.; Feintzeig, I.D.; Salant, D.J. Complement-induced glomerular epithelial cell injury. Role of the membrane attack complex in rat membranous nephropathy. *J. Clin. Investig.* **1986**, *77*, 1096–1107. [CrossRef] [PubMed]
51. Kerjaschki, D.; Schulze, M.; Binder, S.; Kain, R.; Ojha, P.P.; Susani, M.; Horvat, R.; Baker, P.J.; Couser, W.G. Transcellular transport and membrane insertion of the C5b-9 membrane attack complex of complement by glomerular epithelial cells in experimental membranous nephropathy. *J. Immunol.* **1989**, *143*, 546–552. [CrossRef] [PubMed]
52. Schulze, M.; Donadio, J.V.; Pruchno, C.J.; Baker, P.J.; Johnson, R.J.; Stahl, R.A.; Watkins, S.; Martin, D.C.; Wurzner, R.; Gotze, O. Elevated urinary excretion of the C5b-9 complex in membranous nephropathy. *Kidney Int.* **1991**, *40*, 533–538. [CrossRef] [PubMed]
53. Deshmukh, A.B.; Patel, J.K.; Prajapati, A.R.; Mishra, B. Investigating the effect of $CoCl_2$ administration on diabetic nephropathy and associated aortic dysfunction. *Kidney Blood Press. Res.* **2012**, *35*, 694–697. [CrossRef] [PubMed]
54. Detsika, M.G.; Duann, P.; Lianos, E.A. HO-1 expression control in the rat glomerulus. *Biochem. Biophys. Res. Commun.* **2015**, *460*, 786–792. [CrossRef] [PubMed]
55. Muhoberac, B.B.; Hanew, T.; Halter, S.; Schenker, S. A model of cytochrome P-450-centered hepatic dysfunction in drug metabolism induced by cobalt-protoporphyrin administration. *Biochem. Pharmacol.* **1989**, *38*, 4103–4113. [CrossRef] [PubMed]
56. Galbraith, R.A.; Kappas, A. Regulation of food intake and body weight by cobalt porphyrins in animals. *Proc. Natl. Acad. Sci. USA* **1989**, *86*, 7653–7657. [CrossRef] [PubMed]
57. Smith, T.J.; Drummond, G.S.; Kappas, A. Cobalt-protoporphyrin suppresses thyroid and testicular hormone concentrations in rat serum: A novel action of this synthetic heme analogue. *Pharmacology* **1987**, *34*, 9–16. [CrossRef] [PubMed]